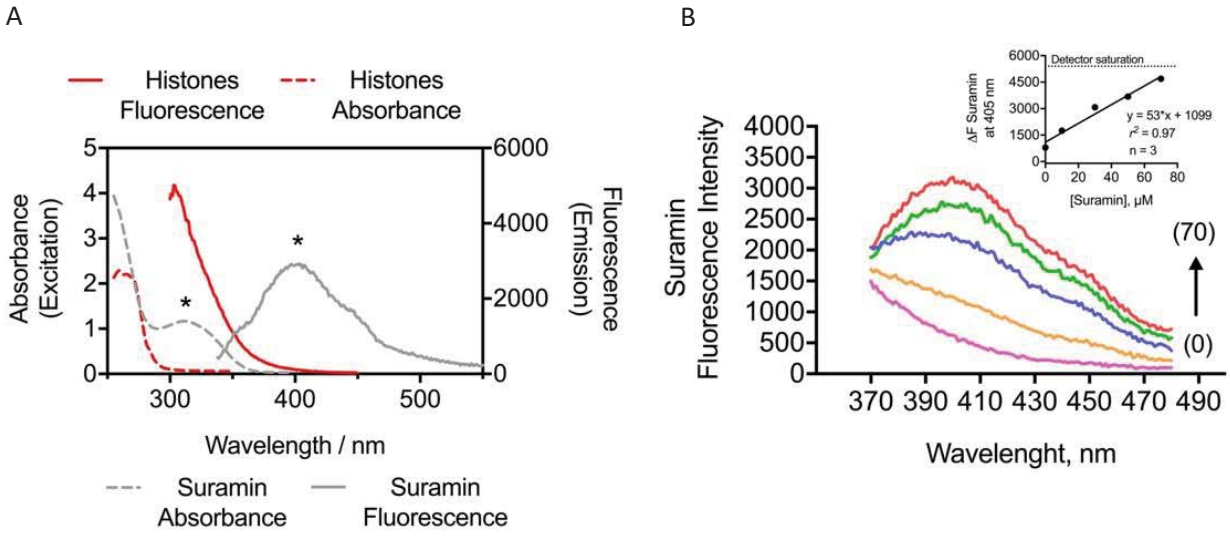

Supplemental Figure 1. Emission (—) and excitation (- - -) spectra of suramin (*) and histones in HEPES buffer (pH 7.4). λ_{exc} = 315 nm and λ_{em} = 405 nm were used for the emission and excitation scan, respectively, of suramin fluorescence, whereas λ_{exc} = 278 nm and λ_{em} = 305 nm were used for the emission and excitation scan, respectively, of histones. (A) Dual plot of both histones and suramin fluorescence and absorbance. (B) Suramin intrinsic fluorescence intensity in solution from 0 (0) to 70 µM (70).

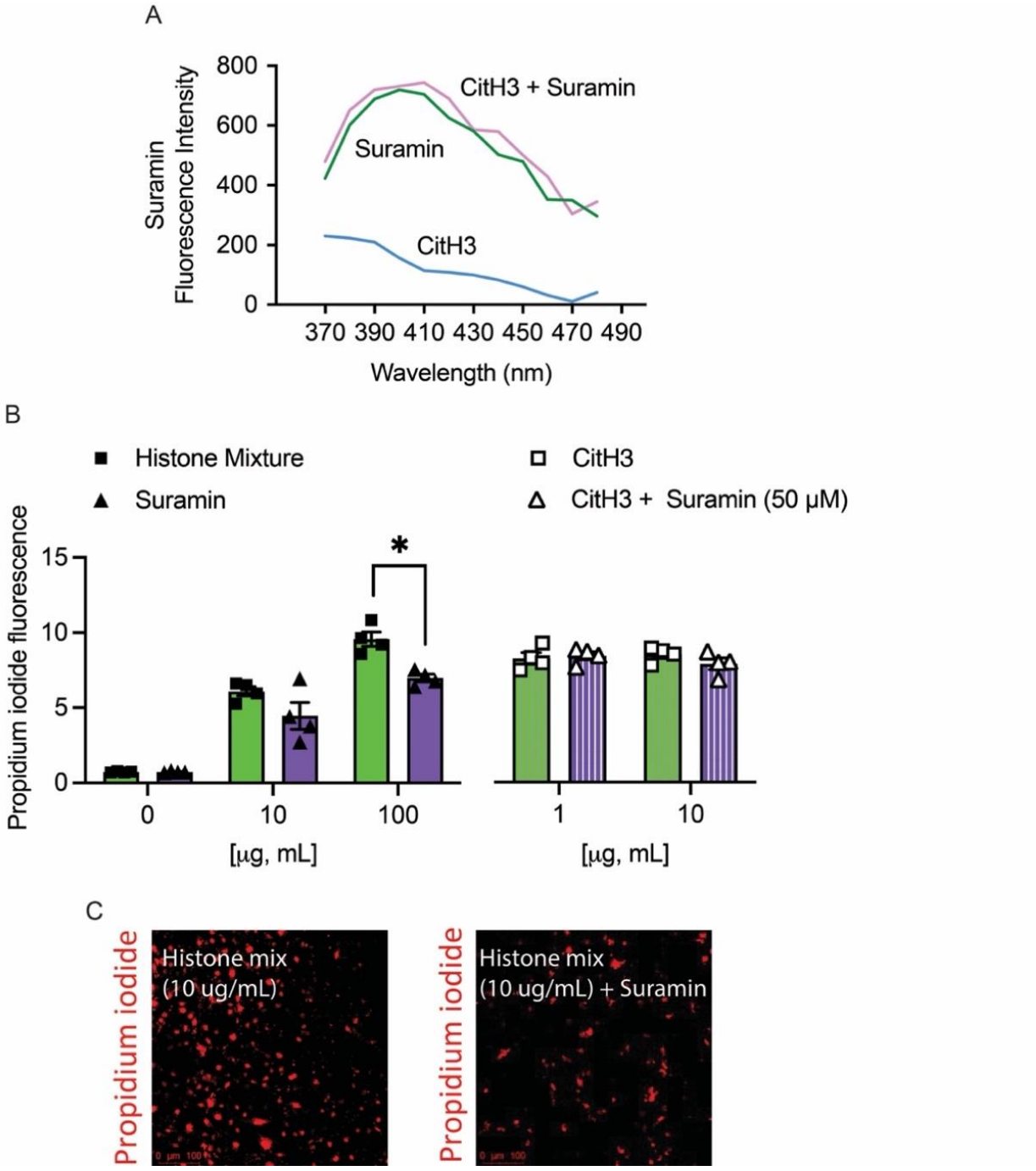

Supplemental Figure 2. Suramin does not bind to citrullinated histone H3. (A**)** *In vitro* fluorescentspectroscopy studies were used to biochemically establish the interaction between suramin (50 µM) and citrullinated histone H3 (1 µg/mL). (B) Lung mouse microvascular endothelial cell death induced by histones (1, 10 and 100 µg/mL) and citrullinated histone H3 (1 and 10 µg/mL) assessed by PI staining (n=4). Two-way ANOVA with Bonferroni's correction for multiple comparisons; $P<0.05$. (C) Representative confocal images of PI stanning of Lung mouse microvascular endothelial cells exposed to histone mixture and histones + suramin.

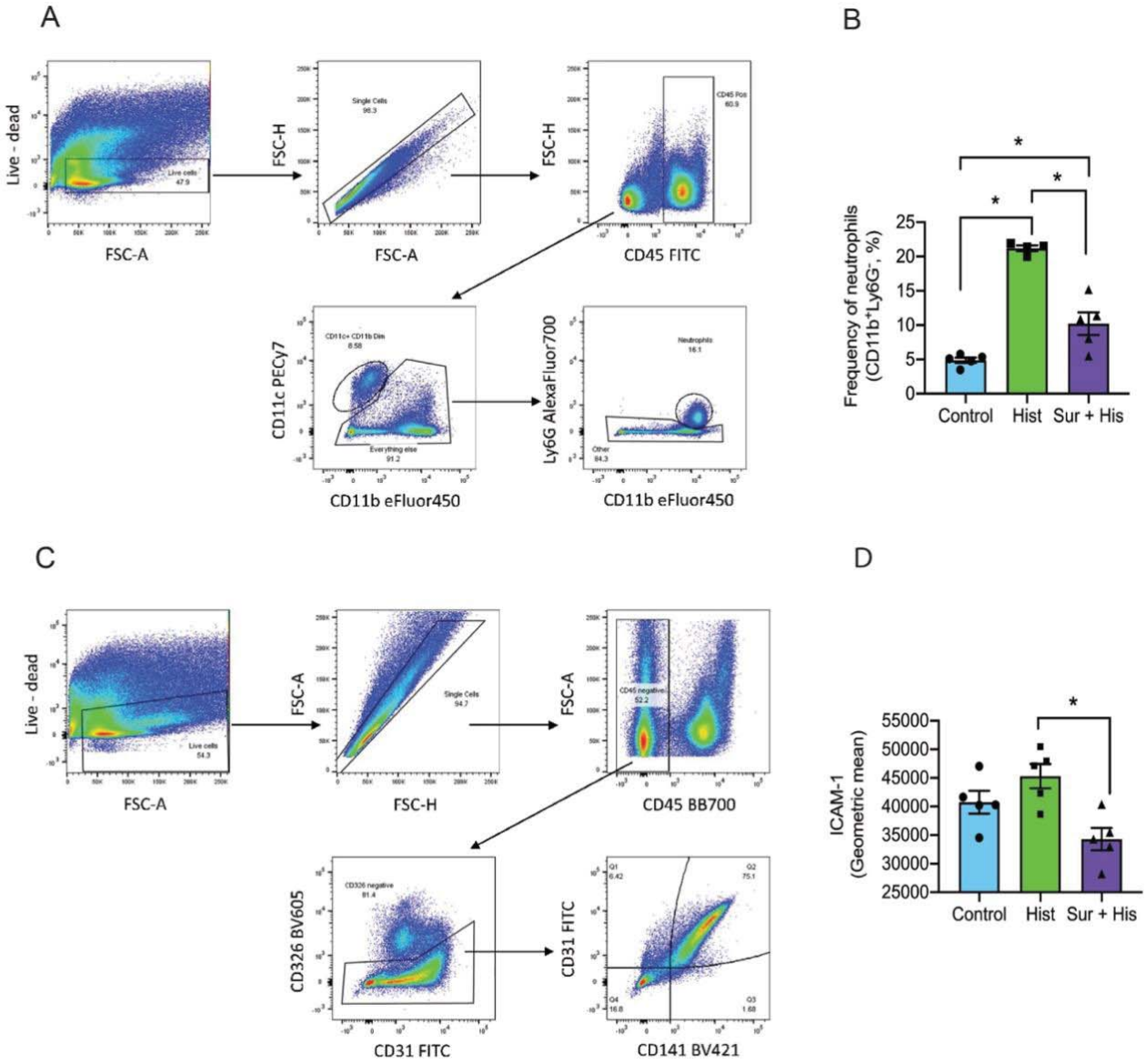

Supplemental Figure 3. Histone-induced neutrophil recruitment and adhesion molecule expression is blocked by suramin. (A) Live cells were gated and doublets excluded (FSC-A vs FSC-H). $CD45^+$ cells were selected and $CD11c^-$ cells identified. Neutrophils ($CD11b^+Ly6G^+$) were identified, and the frequency of neutrophils per live cells determined. (B) Summary data of the frequency of neutrophil levels in lung tissue 4 hours after saline (Control; 300 µL; 4.8 ± 0.4 frequency; n=5), histones (Hist; 45 mg/Kg; 21 ± 0.4 frequency; n=4), or suramin (50 mg/Kg) and histone injection (Sur+His; 10 ± 1.6 frequency; n=5). (C) Live cells were gated and doublets excluded (FSC-H vs FSC-A). $CD45^-$ cells were selected and $CD31^+CD326^-$ cells identified. Endothelial cells ($CD31^+CD141^+$, Q2) were assessed for CD54 expression (geometric mean intensity). (D) Summary data for endothelial ICAM-1 (CD54) expression geometric means (GM) in lung tissue 4 hours after saline (Control; 40743 ± 1999 GM; n=5), histones (Hist; 45 mg/Kg; 45314 ± 2126 GM; n=5), or suramin (50 mg/Kg) and histone injection (Sur+His; 34288 ± 1957 GM; n=5). Data are expressed as mean ± SEM. Two-way ANOVA with Bonferroni's correction for multiple comparisons; $P<0.05$. A new biological replicate culture well was used for each group.

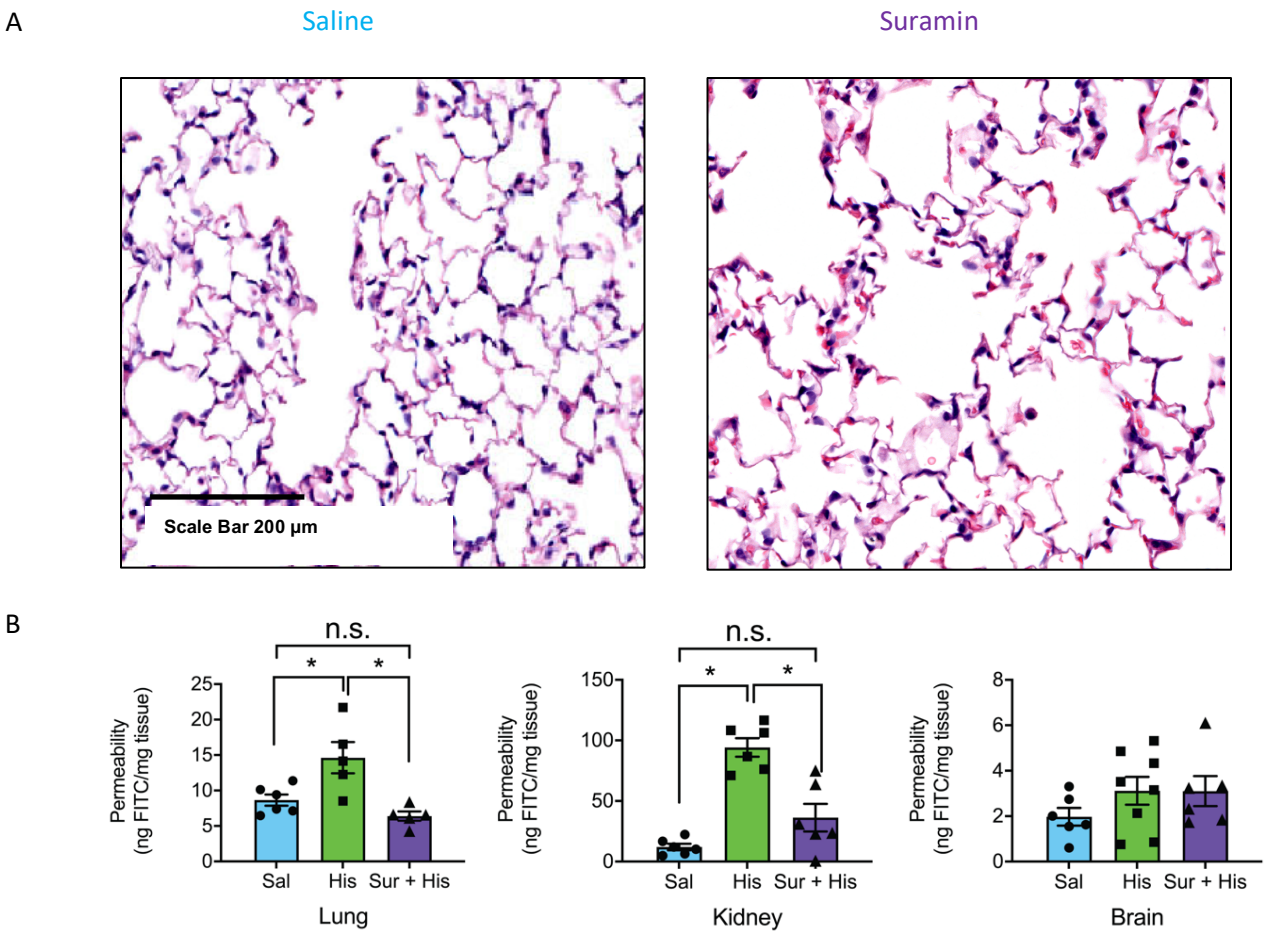

Supplemental Figure 4. (A) Representative images of hematoxylin and eosin stain (H&E) of a histological section of paraffin-embedded fixed lung tissue from mice treated with saline or suramin. The dark blue color denotes cell nuclei, light pink extracellular matrix, and the red erythrocytes. Scale bar = 200 µm. (B) Summary data for FITC-dextran extravasation using the modified Mile's Assay in lung, kidney, and brain tissue from saline (control), histones (45 mg/Kg) and suramin (50 mg/Kg) and histone (Sur+His) injected mice at 4 hr. Lung permeability in saline (control; 8.7 ± 0.8 ng FITC/mg tissue; n=6), histones (His; 14.6 ± 2.2 ng FITC/mg tissue; n=5), and suramin and histone (Sur+His; 6.4 ± 0.7 ng FITC/mg tissue; n=5) injected mice. Kidney permeability in saline (control; 12 ± 2.7 ng FITC/mg tissue; n=6), histones (His; 94 ± 7.7 ng FITC/mg tissue; n=6), and suramin and histone (Sur+His; 36 ± 11 ng FITC/mg tissue; n=6) injected mice. Brain permeability in saline (control; 1.9 ± 0.4 ng FITC/mg tissue; n=6), histones (His; 3.1 ± 0.6 ng FITC/mg tissue; n=6), and suramin and histone (Sur+His; 3.1 ± 0.6 ng FITC/mg tissue; n=6) injected mice. Data are expressed as mean ± SEM. Two-way ANOVA with Bonferroni's correction for multiple comparisons; $P<0.05$. A new biological replicate culture well was used for each group.